https://doi.org/10.48048/tis.2024.8149

Silver Nanoparticles with Modified Synthesis Use Sodium Borohydride Reducing Agent and Okra (*Abelmoschus Esculentus* L.) Raw Polysaccharide Extract as an Anti-Colon Cancer

Ally Kafesa[1,2], Win Darmanto[2,*] and Sri Puji Astuti Wahyuningsih[2]

[1]*Medical Laboratory Technology study program, Faculty of Health, Rajawali Health of Institute, Bandung, Indonesia*
[2]*Doctoral Program of Mathematics and Natural Science, Faculty of Science and Technology, University of Airlangga, Indonesia*

([*]Corresponding author's e-mail: windarmanto@fst.unair.ac.id)

Received: 3 March 2024, Revised: 25 March 2024, Accepted: 2 April 2024, Published: 10 October 2024

Abstract

Nanomedicine using nanoparticles has become a new trend in the treatment of colon cancer. Nanosilver is known to have antibacterial, antifungal, antidiabetic, and anticancer properties. The most common and easy way to make nanosilver is using the reducing agent sodium borohydride, but this inorganic compound element has high toxicity to the body. Polysaccharides have long been known as anticancer agents with low toxicity and few side effects. Okra (Abelmoschus esculentus L.), a flowering plant from the Malvaceae family found in tropical and subtropical areas, and the crude polysaccharide extract from the pods has the highest polysaccharide content. This research aims to determine the effect of raw okra polysaccharide extract (ORPE) as a reducing agent for making nanosilver on its ability as an anti-colon cancer cell line HCT 116. Experiments were carried out by modifying and optimizing the manufacture of AgNPs by reducing $NaBH_4$ with ORPE, 16 concentrations each with repetition 3 times. Characteristic tests were carried out using UV-Vis Spectrophotometry, Particle Size Analyzer, Scanning Electron Microscopy, Transmission Electron Microscopy, cell viability testing with MTT assay, and evaluation of potential apoptosis and necrosis using Annexin V-PI flow cytometry. PSA test for average particle size. Two groups 1 (AgNP-$NaBH_4$) and 2 (AgNP-ORPE) each had repeated measurements 3 times in 16 concentrations. The mean PSA test and zeta potential value for group 1 = 232.5 ± 25.47 nm / –42.23 ± 1.45 mV and 2 = 779.66 ± 112.45 nm / –23.15 ± 3.65 mV. TEM showed that the size of Group 1 was 50.85 nm (χ = 113.14 nm) and Group 2 was 121.43 nm (χ = 248.52 nm). SEM showed that the morphology of both groups was round in shape (group 2 with slight agglomeration). The absorbance spectrum is formed at a wavelength of 389 nm (group 1) and 281.5 nm (group 2). The IC50 value obtained by group 1 = 76.68 mmol/L with 60.3 % apoptotic cells, 3.74 % necrosis and group 2 = 92.58 mmol/L with 81.4 % apoptotic cells and 4.95 % necrosis. ORPE as a nanosilver-reducing agent has been proven to have the potential to induce cell death and cause changes in mitochondrial membrane permeability in the intrinsic pathway of apoptosis.

Keywords: Nanosilver, $NaBH_4$, Okra Raw Polysaccharide Extract (ORPE), HCT 116, Apoptosis, Necrosis, Anticancer

Introduction

Colorectal cancer is a malignant condition that originates from the colon tissue, consisting of the colon (the longest part of the large intestine) and/or the rectum (the last small part of the large intestine before the anus) [1,2]. As is known, colon cancer arises due to abnormal and uncontrolled cell division [3]. Colon cancer is a disease that can arise through 3 main pathways, including sporadic, hereditary and inflammatory cancer. This type of cancer is one of the 3rd most common causes of death in the world [2]. In 2018, the number of colon cancer cases was 1,849,518 cases and 881,000 deaths [4]. This figure represents 10.2 % of all cancer cases in the world. In 2020, cases of death due to colon cancer showed an increasing trend in the incidence of colon cancer in women and men. Evidence from epidemiological studies shows that the rate of colon cancer cases is 10 % and the death rate due to colon cancer is 9.4 % with the majority of men being at high risk [3].

Various treatment efforts have been carried out by experts in the fields of health and biotechnology. Efforts that are now generally applied in health facilities are chemotherapy. Chemotherapy is a therapeutic method in the treatment of colon cancer patients [5,6] and is often combined with immunotherapy such as oncolytic virotherapy, cancer vaccines, cellular immunotherapeutic drugs, immunomodulatory treatments for T cells, and immune checkpoint inhibitors [7]. In addition, as a preventive measure, dimerization can be carried out with antibodies against epidermal growth factor receptors (EGFR-Mab) such as IMC-C_{255}, ABX-EGF, EMD, hR_3 and ICR_{62} [8]. However, the application of therapeutic drugs has several limitations, such as hemopoietic suppression, limited efficacy, immunotoxicity, and drug resistance [1]. This condition has encouraged researchers to develop anticancer drugs with minimal side effects and high effectiveness. Kim *et al.* [6] have studied the impact of using red ginseng in colon cancer chemotherapy and the results show a positive impact. Apart from that, many other studies examine similar things, such as the use of Binahong leaves (*Anredera cordifolia* (Tenore) Steenis) by Lakshita or Melinjo plants (*Gnetum gnemon* L.) by Octavia [10-11]. Many other studies have also examined the use of biomarkers in colon cancer therapy [12-14].

Apart from that, researchers have long been making innovations in the use of polysaccharides as anti-cancer agents. Polysaccharides have long been known as anticancer agents with low toxicity and few side effects [2]. Recently, there has been a shift of interest from microbial polysaccharides to plant polysaccharides due to the lower toxicity and side effects of the latter encapsulated in nanoparticle form. Rapidly developing nanomedicine holds great promise in fighting cancer. Modern medicine has been enhanced by the innovation of metal nanoparticles (NPs) due to their unusual properties that influence their method of action. Silver nanoparticles have been reported to have antibacterial activity [16], anti-cancer [17] and immunomodulator [18]. Polysaccharides from plant extracts are a clean, environmentally friendly, and cost-effective method for producing silver nanoparticles (AgNPs) compared to other chemical and physical methods [19].

The choice of nanoparticle manufacturing method is highly dependent on the polymer and molecular properties. Conventionally, nanoparticles are made using 2 methods, namely polymerization of synthetic monomers and the dispersion of synthetic polymers [20]. One of the most popular methods to synthesize silver nanoparticles is to use cold sodium borohydride to reduce silver nitrate. A large excess of sodium borohydride is required both to reduce ionic silver and to stabilize the formed nanoparticles [21]. Sodium borohydride or sodium tetrahydroborate is a powerful chemical-reducing agent used in various industries such as in the synthesis of medicinal products, the textile sector, or in waste processing. This is the agent of choice for organic substrates because of its ease of consumption, efficiency of use, and its strength as an electron donor so it does not require heating in making AgNPs. Heating has the potential to increase the

agglomeration of particles formed. Polysaccharides have oxidizing properties [22] so they can be used as a substitute for the inorganic compound sodium borohydrate which is easily corrosive and flammable.

Many types of plants are used as sources of polysaccharides. However, several plants have great potential because of their abundance of polysaccharides, one of which is Okra (*Abelmoschus esculentus* L.). Okra is a flowering plant from the Malvaceae family that is found in tropical, subtropical and warm climates throughout the world [23-25]. The pods are rich in polysaccharides, vitamin C, secondary metabolites, minerals and fibre, but low in calories. Apart from being consumed as food, okra is also used as a traditional medicine to treat dysentery and diarrhea. Flavonoid compounds such as catechin oligomers, quercetin, and vitamin C are antioxidants [24-27]. Wahyuningsih *et al.* [28] found that okra polysaccharides act as immune modulators by increasing B lymphocyte proliferation and spleen weight through activation of the transcription factor NFκB. Okra crude polysaccharide extract exerted anticancer effects on Huh7it cancer cells by significantly reducing cell proliferation and inducing cell apoptosis. With the results of these studies, it appears that raw okra polysaccharide extract has the potential to be useful for the management of colon cancer patients. This ability can be used as a new mechanism for treating colon cancer based on nanoparticles.

This research was conducted to develop innovations in nanoparticle-based colon cancer treatment using silver. A trend that is currently being developed by researchers in the health sector. In developing nano silver, modifications were made using sodium borohydrate as a reducing agent and Okra extracts as an anti-cancer. The research focused on several things, namely 1) physical characterization of the nanoparticles being developed and 2) testing their effectiveness as anti-cancer drugs.

Materials and methods

This research was carried out experimentally to make a nanosilver with the reducing agents $NaBH_4$ and ORPE with 16 concentrations each and repeated 3 times incubation of 24, 48 and 72 h. The cell incubation period was performed with an AgNP concentration from 0.1, 0.5, 1, 2.5, 5, 7.5, 10, 20, 30, 40, 50, 60, 70, 80, 90, 100 mmol/L [29].

Research was carried out to determine the characteristics of the nanosilver formed using PSA, SEM, and TEM tests [3]. Colon anti-cancer potential was tested using a cell viability test (cytotoxic test) with interpretation of IC_{50} results using SigmaPlot and the Constant Variance Test (Spearman Rank Correlation) statistical test as well as evaluating the ability of apoptosis and necrosis using the flow cytometry test [2].

Tools and materials

The materials used in this research were Silver nitrate (Sigma Aldrich, ReagentPlus®, ≥ 99.0 % (titration)), polyvinylpyrrolidone (Sigma Aldrich, Cas. Number 9003-39-8, PVP10), Sodium Borohydride (Sigma Aldrich, powder ≥ 98.0 %, Cas. Number 16940-66-2), Natrium Chloride (Merck IC Standard, 1.19897.0500), Deionized (DI) water was used for all experiments. Pods of Abelmoschus esculentus L. (Certified by Biosystematics and Molecular Laboratory, Herbarium Padjadjaran University), FITC annexin V (Invitrogen, USA, 25 mM HEPES, 140 mM NaCl, 1 mM EDTA, pH 7.4, 0.1 % bovine serum albumin), Propidium iodide (Invitrogen, USA, 1 mg/mL PI (1.5 mM) solution in deionized water), 5X annexin-binding buffer (Invitrogen, USA, 50 mM HEPES, 700 mM NaCl, 12.5 mM CaCl2, pH 7.4), RPMI-Medium 1640 (Merck, R0883), Fetal Bovine Serum (Merck, 12106C), Trypsin EDTA 0.05 % (Merck,T4049), Phosphate Buffer Saline (Merck, P2272, pH 7.2), MTT assay (Merck, No.114650007001), Cell line colon cancer HCT 116 (ATCC, CCL 247). Meanwhile, the equipment used in this research was a Microscope (Olympus), UV-Vis Spectrophotometer (Thermo Scientific, Multiskas Ex), Flow cytometer (BD

FACSLyricTM), Scanning Electron Microscope (Bronchure, SU3500), Transmission Electron Microscope (Hitachi TEM System, HT7800), Particle Size Analyzer (Horiba Scientific, SZ-100).

Research procedure

There are several stages carried out in this research, namely 1) making Okra Raw Polycarcass Extract (ORPE); 2) nanosilver synthesis; 3) identifying the characteristics of nanosilver; 4) HCT-116 colon cancer cell culture; 5) colon cancer cell viability test; and 6) evaluation of potential apoptosis and necrosis.

Making okra raw polysaccharide extract (ORPE)

Okra fruit was obtained from traditional markets in Surabaya, Indonesia. Fresh okra fruit (500 g) was cleaned with water, cut into pieces, mashed, and macerated with 500 mL of distilled water 3 times overnight. The supernatant was collected and centrifuged at 4,300 rpm for 5 min. The supernatant was precipitated in 1× the sample volume of absolute ethanol, incubated for 24 h at 4 °C and centrifuged. The pellet was dissolved in distilled water and centrifuged. The supernatant was collected and lyophilized [4]. The raw polysaccharide powder from okra fruit is called Okra Raw Polysaccharide Extract (ORPE).

Synthesis of nanosilver

With reducing agent Sodium Borohydrate

Add 30 mL of 0.002 M sodium borohydride ($NaBH_4$) to the Erlenmeyer flask. Add a magnetic stir bar and place the flask in an ice bath on a stir plate. An ice bath is used to slow the reaction and provide better control over the final particle size/shape. Stir and refrigerate the liquid for about 20 min. Drop 2 mL of 0.001 M silver nitrate ($AgNO_3$) into the $NaBH_4$ solution stirring at a rate of about 1 drop per second. Stop stirring immediately after all the $AgNO_3$ has been added. By mixing the 2 solutions (namely $NaBH_4$ and $AgNO_3$). The addition of a few drops of 1.5 M sodium chloride (NaCl) solution causes the suspension to turn dark yellow, then grey as nanoparticle aggregates. Add a drop of Polyvinylpyrrolidone (PVP) 0.3 %. PVP prevents aggregation. The addition of the NaCl solution then did not affect the color of the suspension [5].

With ORPE

500 mg of okra extract was dissolved in 100 mL of distilled water. Next, 30 mL of extract was added to 2 mL of 0.1 mM $AgNO_3$ solution. Then several drops of 1.5 M NaCl and 1 drop of 30 % PVP [5]. After 24 h of incubation, the solution will turn dark brown, indicating the formation of silver nanoparticles. The solution was then transferred to a water bath and heated at 90 °C. After 15 min, centrifugation was carried out at room temperature at a speed of 9,000 rpm. The centrifuged pellet was then washed with distilled water several times and dried in an oven at 80 °C to obtain a blackish powder [6].

Characteristics of nanosilver

A scanning electron microscope (SEM) was used to analyze the surface morphology of biosynthetic silver nanoparticles (AgNPs). Meanwhile, the remaining unused nanoparticle biosynthesis was stored in 0.9 % saline for further characterization. The size of the nanoparticles and their surface tension were measured using a Particle Size Analyzer (Zetaisher Nano ZS) at 25 °C with a detection angle of 90 °C. Transmission Electron Microscope (TEM) is used to visualize the smallest structure of the silver nanoparticles formed [7].

HCT-116 colon cancer cell culture

Colon cancer cells (HCT-116) were grown in RPMI-1640 media in 75 cm^2 flasks supplemented with fetal bovine serum (10 %, FBS), sodium pyruvate (1 mM), L-glutamine (2 mM), and antibiotics (penicillin 100 IU/mL, streptomycin 100 µg/mL) under standard conditions (37 °C, air humidity 95 and CO_2 5 %) [8].

Colon cancer cell viability assay

The cytotoxicity of AgNP-ORPE was determined using the MTT assay. HCT 116 colon cancer cells were seeded into 96-well plates at a density of 1×104 cells/well. Cells were treated with 1 - 100 µg/mL AgNP-ORPE for 24, 48, and 72 h. Next, MTT was added to the wells and incubated for 4 h. The mixture of extract and MTT was removed and replaced with 200 µL/well DMSO. Absorbance values were measured at 550 nm [9].

Evaluation of potential apoptosis and necrosis

Colon cancer cells that had been treated with AgNP-ORPE were stained with Annexin V-FITC and propidium iodide (PI) at room temperature for 20 min. Next, apoptotic and necrotic cells were analyzed by flow cytometry [10].

Results and discussion

Nanosilver synthesis results

The $AgNO_3$ solution reacted with sodium borohydrate ($NaBH_4$) and ORPE has a brownish-yellow and slightly light-yellow color. The color formation results from colorless to brownish yellow and light yellow which is an indication that silver nanoparticles have been formed. The success of the synthesis of silver nanoparticles using reducing and stabilizing agents sodium borohydrate and PVP can be seen from the appearance of absorbance peaks in the wavelength range of 350 - 450 nm. Based on the results, neither the $AgNO_3$ solution nor the sodium borohydrate solution has an absorption peak at a wavelength of 350 - 450 nm, which indicates that silver nanoparticles have not yet been formed. Meanwhile, the absorbance spectrum is formed at a wavelength of 389 nm which shows the formation of new components in the form of silver nanoparticles after the $AgNO_3$ solution and sodium borohydrate solution are reacted. In the synthesis of AgNP-ORPE, there was a difference in the maximum absorption of the nannosilver that was produced, a peak absorption was obtained at 281.5 nm as in **Figure 1**.

The results of testing for particle size, polydispersity index, and zeta potential of AgNP were carried out 3 times and the average results are presented in **Table 1**. Based on the PSA test data, it is known that AgNP-$NaBH_4$ has a smaller average particle size than AgNP-ORPE and with the same equipment. You can also observe the AgNP polydispersity index value. The size of AgNp-$NaBH_4$ particles has a size distribution of 40 - 100 ± 2 nm (10 %), 340 - 650 ± 11 nm (37 %) and ≥ 1,000 nm (53 %) (**Figure 2(a)**) while the size distribution of AgNP-ORPE particles starts from 584 - 788 ± 21 nm (75 %) and ≥ 1,000 nm (25 %) (**Figure 2(b)**). The size of the particles formed is influenced by the zeta potential value so that the stability of the degree of coagulation of each product experiences quite large agglomerations (**Table 1**). There is a significantly repulsive electrostatic contact between particles when they have a substantially positive or strongly negative zeta potential. By doing this, the particles are kept from becoming too near to one another and clumping together. Van der Waals forces (Φ_A) which are based on dipole-dipole interactions (Φ_R) come into play when particles are near to one another, according to DLVO theory. There is an allure to these powers. The electrical double layer has less of a repulsive impact and increases the likelihood of coagulation at zeta potentials around 0. Zeta potential is measured in millivolts and is typically found in the –200 mV

to +200 mV range. Although it can be used to forecast stability, the zeta potential cannot be used to assess the stability of a dispersion directly. The zeta potential is typically used to evaluate the quality of the dispersion because it is much simpler and quicker to analyze than a stability measurement. A common way to characterize nanoparticle stability is in terms of the particular size-dependent quality that is used in a given application. The preservation of metal surface area was connected to nanoparticle stability, and this in turn was connected to a lower likelihood of nanostructure aggregation. Pd nanoparticles stabilized by PAMAM dendrimer demonstrated the highest catalytic activity, which was surpassed by those stabilized by block copolymer and PVP. This result implies that the maintenance of a primary, non-aggregated particle state is connected to nanoparticle stability [34].

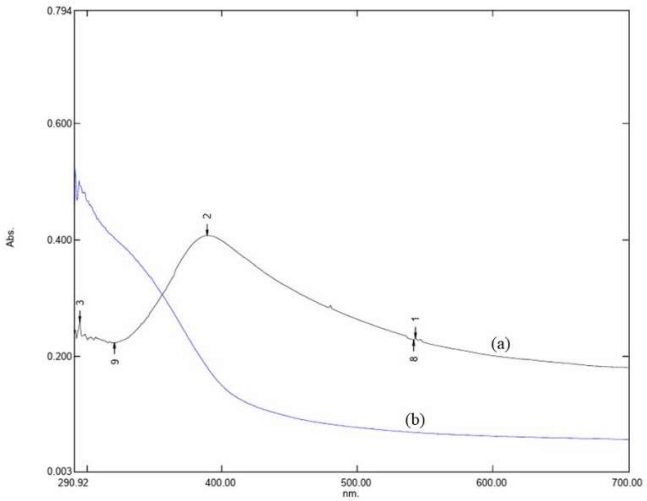

Figure 1 Uv-vis spectrum of Nanosilver. (a) AgNP-$NaBH_4$ and (b) AgNP-ORPE.

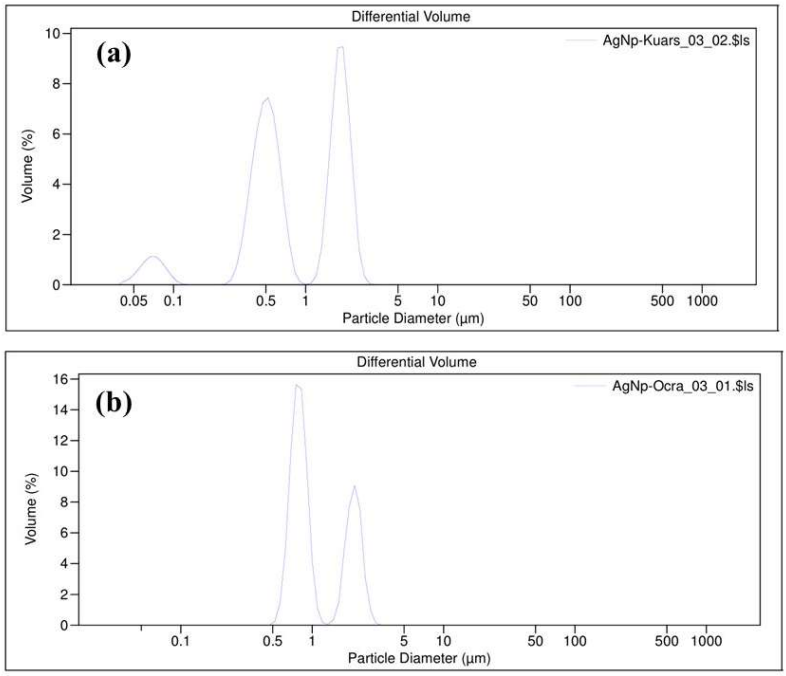

Figure 2 Distribution of AgNP PSA assays. (a) AgNP-$NaBH_4$ and (b) AgNP-ORPE.

Based on **Table 1**, the measurement of the zeta potential value of AgNP-$NaBH_4$ has a fairly wide range with AgNP-ORPE. The Polydispersity Index (PDI) is almost the same for both, it is expected that its hydrodynamic diameter will be larger than that of the core because it includes a surface coating material and a solvent layer that adheres to the surface of the particle when it moves under the influence of Brownian motion [11].

Table 1 AgNP PSA test results.

Testing	Results (Average ± SD)	
	AgNP-$NaBH_4$	**AgNP-ORPE**
Particle Size	232.5 ± 25.47 nm	779.66 ± 112.45 nm
Polydispersity Index	0.8953 ± 0.001	0.8960 ± 0.002
Zeta Potential	–42.23 ± 1.45 mV	–23.15 ± 3.65 mV

The microscope methods used to characterize particle shape and size are Scanning Electron Microscopy (SEM) and Transmission Electron Microscopy (TEM). This tool contains a 2-dimensional image and is formed from 2 electrons transmitted through the sample. The results of measurements using SEM can be seen in **Figure 3**. It is known that the morphology of AgNP-$NaBH_4$ produced from the synthesis appears clustered and the morphology of AgNP-ORPE appears in pieces.

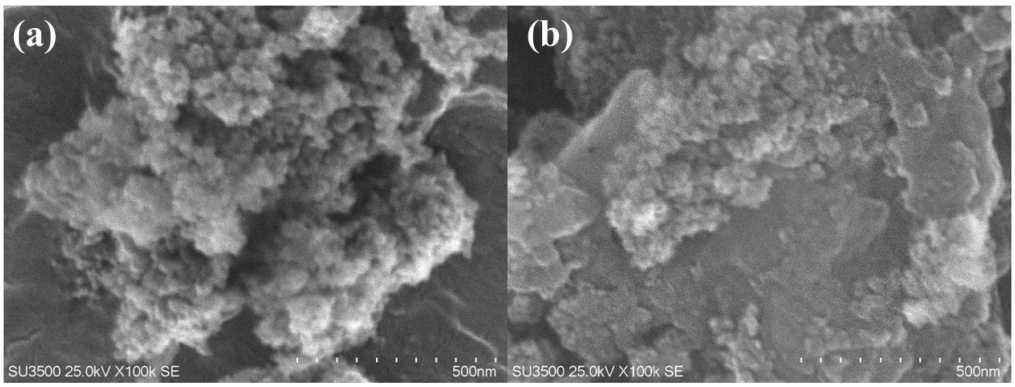

Figure 3 SEM micrographs magnification 100,000×. (a) AgNP-$NaBH_4$ and (b) AgNP-ORPE.

In the SEM results, a bright black/dark white image is obtained which is influenced by the constituent elements at a size of 500 nm. Metal elements with a higher atomic number will give a lighter/whiter color than metal elements with a lower atomic number [11]. The appearance of the particles detected was round in shape with slight agglomeration.

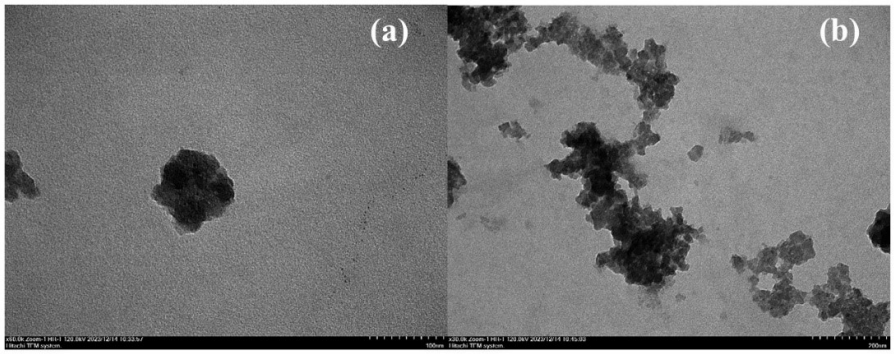

Gambar 4 TEM 120.000× (a) AgNp-$NaBH_4$ and (b) AgNp-ORPE.

The results of measurements using TEM can be seen in **Figure 4**. It is known that the morphology of AgNP-NaBH4 produced from the synthesis appears spherical and the morphology of AgNP-ORPE appears to be round with pieces/asymmetric. In this tool, the ImageJ Application was used to determine the particle size, and the results obtained were that the smallest size of AgNP-$NaBH_4$ was 50.85 nm with an average size of 113.14 nm and the smallest size of AgNP-ORPE was 121.43 nm with an average size 248.52 nm.

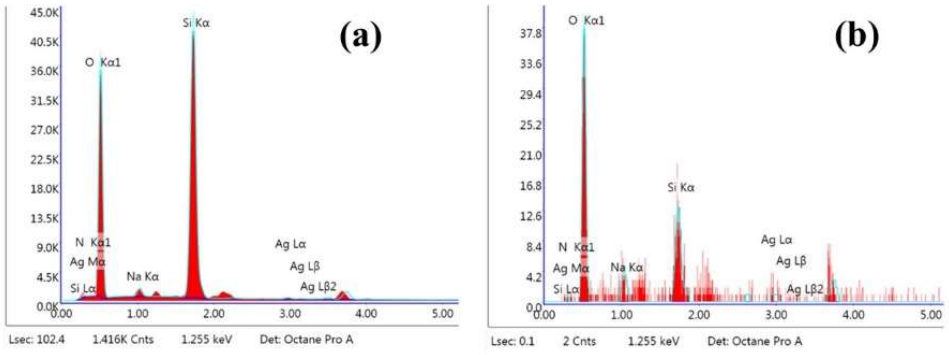

Figure 5 Energy-dispersive X-ray spectroscopy testing. (a) AgNP-$NaBH_4$ and (b) AgNP-ORPE.

In the EDX test, firing was carried out at the desired point/spot on the nanosilver matrix and 6 elements that made up AgNP were found as shown in **Table 2**. The percentage of the most dominant element was oxygen, followed by silica, then Ag. The silver element formed is influenced by the concentration of Ag used so the nanosilver formed uses more $NaBH_4$ (1.22 %) than ORPE (0.21 %).

Table 2 EDX spectrum of AgNPs.

Elements	Sum Spectrum			
	AgNP-$NaBH_4$		AgNP-ORPE	
	Weigth %	Atomic %	Weigth %	Atomic %
N K	0.00	0.00	0.26	0.36
O K	46.30	60.41	62.45	75.70
NaK	1.65	1.45	10.71	9.04
SiK	51.03	37.93	19.81	13.68
AgL	6.78	1.22	1.07	0.21

Anticancer testing results

Based on the results of staining with MTT using 16 concentrations from 0.1 - 100 mmol/L for each AgNP sample, 24 - 48 h of incubation did not show an increase in colon cancer cell death in both treatments. After 72 h of incubation (**Figure 7**), IC_{50} AgNP-$NaBH_4$ was obtained at a concentration of 76.7830 mmol/L and $IC5_0$ AgNP-ORPE at a concentration of 92.5861 mmol/L. This shows that AgNPs have the potential to kill colon cancer cell lines whether made using $NaBH_4$ or ORPE (**Figure 6**). Based on the Constant Variance Test (Spearman Rank Correlation) on SigmaPlot ($p = 0.0783$), the higher the AgNP concentration, the more colon cancer cells will die (**Table 3**).

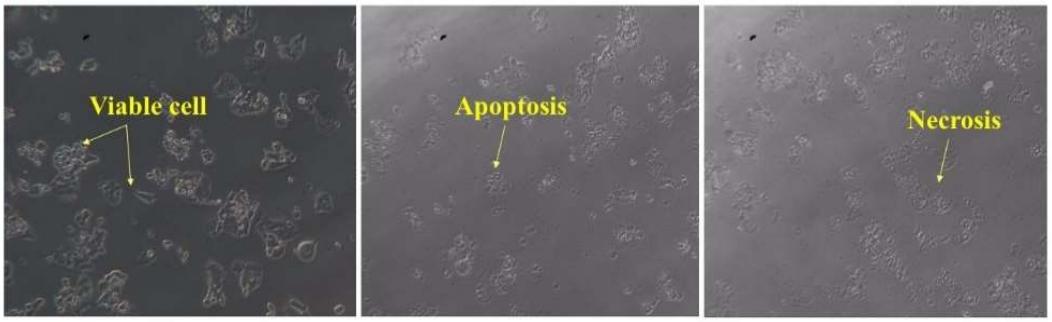

Figure 6 Changes in colon cancer cell line (HCT 116) after 72 h of incubation. (a) RPMI-1640 control medium, (b) addition of AgNP-$NaBH_4$, and (c) addition of AgNP-ORPE.

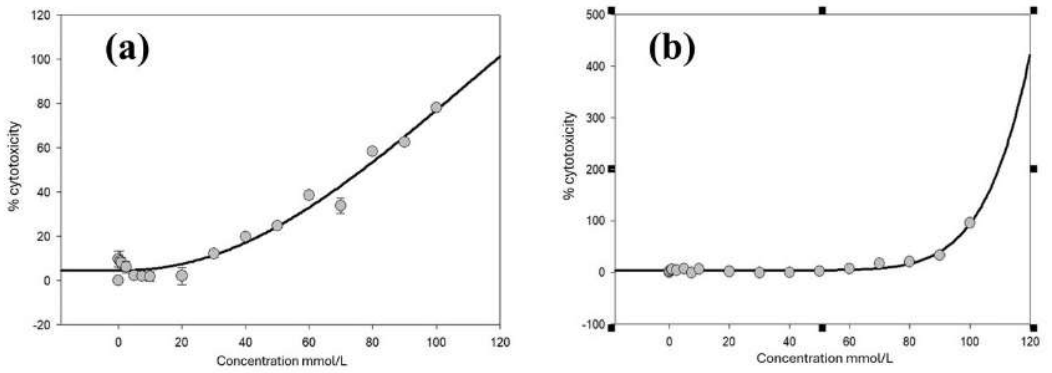

Figure 7 Toxicity test (IC_{50}) using SigmaPlot after incubation for 72 h in RPMI-1640 media; (a) addition of AgNP-$NaBH_4$, (b) addition of AgNp-ORPE.

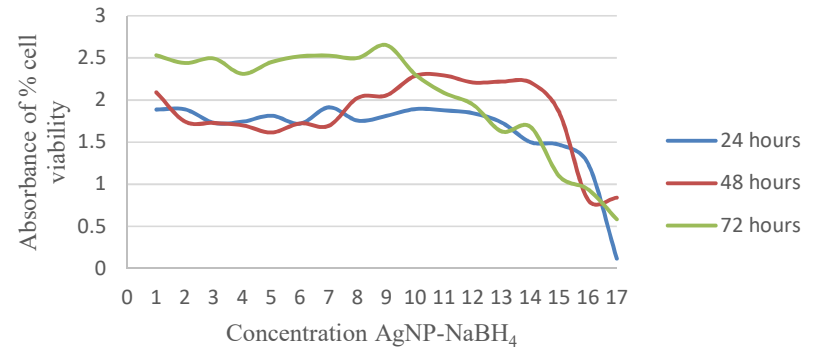

(a)

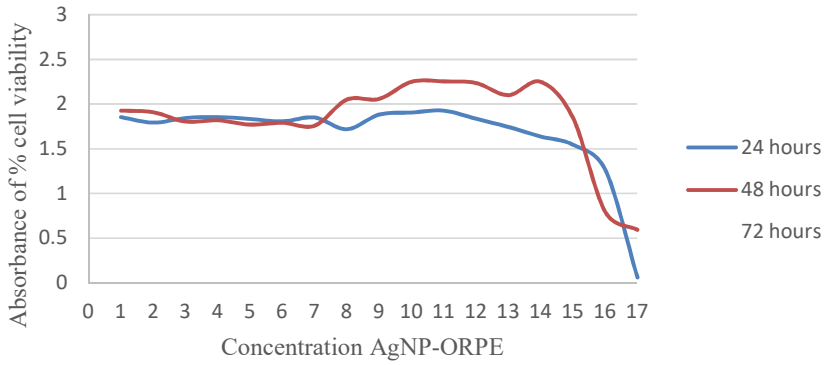

(b)

Figure 8 Percentage absorbance (dose-response) of cell viability HCT 116 human colon cancer cells with MTT assay according to serial concentration of (a) 0.1 - 100 mmol/L AgNP-$NaBH_4$ and (b) 0.1 - 100 mmol/L AgNP-ORPE.

Figure 8(a) illustrates how, at the dose of AgNP-$NaBH_4$ administered to HCT 116 cancer cells, a drop in the absorbance of the percentage of living cells may be seen across many incubation durations with each repetition. According to the MTT staining assay, there are still a lot of live cancer cells present at concentrations between 0.1 and 50 mmol/mL. The curve in AgNP-ORPE (b) displays a similar pattern at values ranging from 0.1 to 40 mmol/mL. After incubating the cells for 24 h, it was not possible to determine the IC_{50} concentration of the 2 sample treatments since cell death only happened at a concentration of 90 mmol/mL (not yet meeting the 50 % mortality requirement). The absorbance of the percentage of living cells in both treatments started to decline at a concentration of 70 mmol/L in the 2nd repetition (48 h of incubation). Calculations for inhibition cannot be performed under these conditions. After 72 h of incubation, 50 % of the cancer cells were found to have died at an initial concentration of 50 mmol/L for AgNP-$NaBH_4$ and 40 mmol/L for AgNP-ORPE. AgNP-$NaBH_4$ 76.6830 mmol/mL and AgNP-ORPE 92.5816 mmol/mL were the IC_{50} values (IC parameter at 50.00) that were determined through calculations using the sigma plot software (**Table 4**). With a significant value at 24 h (p = 0.3636), 48 h (p = 0.3148) and 72 h (p = 0.0783), the p-value for each incubation time has an average of > 0.05, according to the ANOVA test (**Table 3**), which is based on this table above. As a result, the variance of the test choices for both nanoparticle conditions at each various incubation temperature is equal.

Table 3 Statistic analysis of variance.

24 h	DF	SS	MS	Statistical test	
				Normality test (Shapiro-wilk)	**Constant variance test (spearman rank correlation)**
Regression	4	32,923.7741	8,230.9435	• W Statistic = 0.9700 • Passed (p = 0.2215) • Significance level = < 0.0001	Passed (p = 0.3636)
Residual	57	971.1830	20.6635		
Total	41	33,894.9570	664.6070		
Corrected for the mean of the observation;					
Regression	3	25,465.7001	8,488.5667		
Residual	47	971.1830	20.6635		
Total	50	26,436.8831	528.7377		
48 h	**DF**	**SS**	**MS**	**Statistical test**	
				Normality test (Shapiro-wilk)	**Constant variance test (spearman rank correlation)**
Regression	4	23,349.5923	5,837.3981	• W Statistic = 0.9357 • Passed (p = 0.0083) • Significance level = < 0.0001	Passed (p = 0.3148)
Residual	47	5,315.8141	113.1024		
Total	51	28,665.4064	562.0668		
Corrected for the mean of the observation;					
Regression	3	19,486.7100	6,495.5700		
Residual	47	5,315.8141	113.1024		
Total	50	24,802.5241	496.0505		
72 h	**DF**	**SS**	**MS**	**Statistical Test**	
				Normality test (Shapiro-wilk)	**Constant variance test (spearman rank correlation)**
Regression	4	51,476.4330	12,869.1083	• W Statistic = 0.9744 • Passed (p = 0.3341) • Significance level = < 0.0001	Passed (p = 0.0783)
Residual	47	1,030.1787	21.9187		
Total	51	52,506.6118	1,029.5414		
Corrected for the mean of the observation:					
Regression	3	27,597.9446	9,199.3149		
Residual	47	1,030.1787	21.9187		
Total	50	28,628.1234	572.5625		

Tabel 4 Statistic IC_{50} by sigmaplot software.

Sample	IC Paramaeter	Predicted	Residuals	X column	Y column	IC_{50}
AgNP- ORPE	25.00	3.5150	3.5150	–3.5150	3.5150	84.6785
	50.00	6773.9201	3.5150	0.8197	3.5150	92.5816
	75.00	164.0948	3.5150	–1.8984	3.5150	97.3232
	90.00	8.6910	3.5150	–2.5380	3.5150	99.5055
AgNP- $NaBH_4$	25.00	4.3938	–4.3938	–18.000	4.3938	50.8196
	50.00	336.8319	7.6844	–17.4609	4.3938	76.6830
	75.00	182.2377	6.7562	–16.9219	4.3938	98.4244
	90.00	2.1275	2.5415	–16.3828	4.3938	110.7822

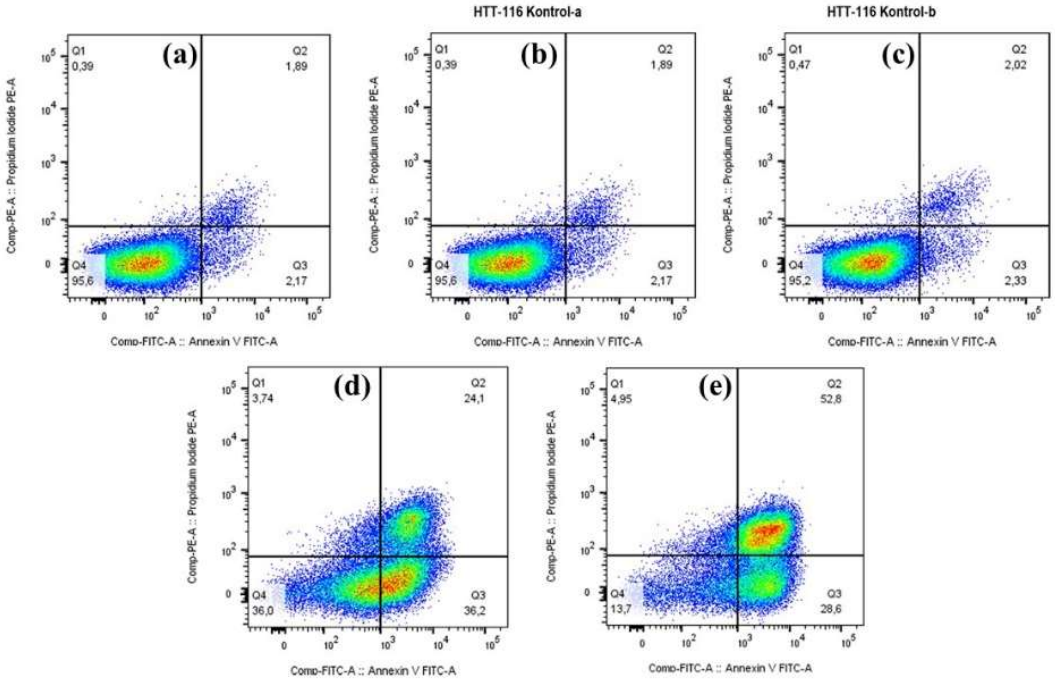

Figure 9 Analysis of HCT 116 cells using flow cytometry after cells were stained with annexin V-FITC and PI. Q1: Necrosis, Q2: Late apoptosis, Q3: Early apoptosis, Q4: Live cells. (a): Normal control, (b): Positive control A (AgNP-$NaHB_4$), (c): Positive control B (AgNP-ORPE), (d): AgNP-$NaBH_4$ 76.68 mmol/L and, (e): AgNP-ORPE 92.58 mmol/L.

The efficacy of AgNP-$NaBH_4$ and AgNP-ORPE on cell apoptosis and necrosis, cells treated with Annexin-V FITC and PI. The percentages of early apoptosis, late apoptosis, and necrosis were measured using flow cytometry. The data are shown in **Figure 9**. The AgNp-$NaBH_4$ group with a concentration of 76.68 mmol/L showed the highest rate of early apoptosis (36.2 %) followed by the AgNP-ORPE group with a concentration of 92.68 mmol/L which caused 28.6 % of cells to undergo premature apoptosis. Meanwhile, the highest level of late apoptosis occurred in the AgNP-$NaBH_4$ group at 24.1 % and AgNP-ORPE at 52.8 %.

Cancer cell death occurs through 2 pathways, namely the extrinsic pathway or death receptor pathway (DR) and the intrinsic pathway or mitochondrial pathway [18]. One of the extrinsic pathways is carried out by NK cells which are part of the innate response which is included in the lymphocyte class. Meanwhile, the mitochondrial pathway involves various groups of proteins such as Bax, Bcl, p53 and the caspase family which can then cause DNA damage and apoptosis in cancer cells [15].

This study found that AgNP-$NaBH_4$ and AgNP-ORPE can reduce the metabolism of colon cancer cells. In AgNP-$NaBH_4$, Ag^+ ions released by AgNP enter the cell. Then they reach the mitochondria where they interact with the thiol group and bind to the NADPH dehydrogenase enzyme and liberate Reactive Oxygen Species (ROS) [36]. The ROS formed in mitochondria interact with enzymes in the respiratory pathway, damaging the formation of ATP and the cell's respiratory cycle. ROS are also formed by interacting with proteins, sulfur and phosphorus-containing cell constituents. Also, these ROS that are formed bind to the phosphorus elements of DNA and RNA which leads to inhibiting cell replication and protein synthesis thereby causing cell death. In AgNP-ORPE, Okra Raw Polysaccharide Extract contains 29.9 % rhamnose [37]. It is known that ORPE has anti-liver cancer abilities [17]. Wahyuningsih *et al.* [18] proved that treatment with ORPE for 48 h resulted in cell accumulation in the G_0/G_1 phase. Cells treated with lower concentrations of ORPE drastically increased the G_0/G_1 Phase sub-population when compared to the control group. Although cell accumulation at each ORPE concentration was dynamic, all groups were found to arrest cells in the G_0/G_1 phase. In the mitochondrial pathway too, apoptosis is caused by the release of cytochrome-c through the formation of channels associated with the mitochondrial permeability transition pore (PTP) and the protein Bax. Cytochrome-c released into the cytosol will form an apoptosome complex together with Apaf-1, ATP and caspase 9. This apoptosome will activate caspase-3 which plays a role in cutting the cytoskeleton and cleavage of gelsolin, a protein involved in maintaining cell morphology until the cell undergoes apoptosis [33]. AgNP-ORPE functions potentially as a mitogen to initiate the process of exogenous apoptosis. The homologous ligands of Fas and TRAILR, respectively, are bound by the former and activated by the latter. As a result of this binding and activation, the receptor tail undergoes conformational changes inside the cell, attracting procaspase-8, long-chain cFLIP, and FADD to create DISC. Procaspase-8 in DISC is activated by cFLIP to caspase 8, and caspase-8 causes apoptosis through either activating executioner caspase-3/7 directly or by cleaving BID into tBID, which then travels to the outer mitochondrial membrane and causes MOMP to form, which in turn causes apoptosis [38].

Inhibition of cancer growth can cause apoptosis, which is programmed cell death of cells [36]. Flow cytometry data showed that the highest level of AgNP-$NaHB_4$ 76.68 mmol/L was able to cause cells to experience the highest early apoptotic phase. Meanwhile, the lowest AgNP-ORPE level of 92.58 mmol/L was able to cause cells to experience the highest late phase of apoptosis. The balance of early and late apoptosis is estimated at AgNP levels of 70 - 80 mmol/L because the distribution of cells that react differently enters the Q2 and Q3 quadrants on the flowcitometry graph. AgNP-$NaBH_4$ with levels of ± 70 mmol/L can react to cancer cells, especially in early apoptosis. It is conceivable that higher AgNP-NaBH4 could help increase the initiation of apoptosis in HCT 116 cancer cells. Likewise, AgNP-ORPE levels have the same potential as levels < 92.58 mmol/L. However, the high number of apoptotic cells in the AgNP-$NaBH_4$ treatment group compared with the AgNP-ORPE group indicated that the caspase family of proteins was being activated.

Administration of AgNP-$NaBH_4$ not only caused 36.2 % of HCT 116 cells to experience early apoptosis and 24.1 % late apoptosis but also caused 3.74 necrosis. Likewise, administration of AgNP-ORPE caused 26.6 % to experience early apoptosis, 2.8 % late apoptosis and 4.95 % necrosis. Necrosis is caused by factors external to the cell or tissue, such as infection, toxins, or trauma that result in irregular digestion of cell components [33]. Although AgNPs have made many advances in the development of new drugs,

toxicity is the most important problem to hinders efficacy/efficiency or causes side effects. The toxicity of AgNPs is closely related to particle size [39]. Most AgNPs are toxic to the human body, and it is precisely because of their small particle size that silver nanoparticles can penetrate human tissue. Zhang *et al*. studied 2 sizes of AgNPs to test differences in neurotoxic effects (20 and 70 nm silver nanoparticles). The results showed that 20 and 70 nm silver nanoparticles significantly reduced nerve cell viability, and 20 nm silver nanoparticles exerted a stronger toxic effect than 70 nm silver nanoparticles. The synthesis of AgNP-ORPE has a zeta potential value (–23.15 ± 3.65 mV) which is lower than AgNP-$NaBH_4$ (–42.23 ± 1.45 mV), thereby increasing Van der Walls forces and agglomeration occurs. This causes a high concentration (> 50 %) of both synthesized AgNPs because it reduces the ability to penetrate tissue. Yuan [36] revealed that a combination treatment of camptothecin and silver nanoparticles significantly increased the number of cancer cells. Overall, these results suggest that camptothecin and silver nanoparticles cause cell death by inducing changes in mitochondrial membrane permeability and caspase activation. Of course, the combination of chemotherapy and silver nanoparticles provides a beneficial effect in cancer treatment compared to immunotherapy. Cells that undergo apoptosis or necrosis show typical changes in their morphological and physical properties (cell shrinkage, chromatin and cytoplasm condensation) which can be measured by microscope observation of the media or by flow cytometry. This research needs to be expanded on the size of the nanosilver formed to obtain better bioavailability. Next, we will study the special DNA peaks that appear when cells undergo apoptosis during the colon cancer cell cycle.

Conclusions

$NaBH_4$ and Okra Raw Polysaccharide Extract (ORPE) have the potential to form nanosilver as a reducing agent and can induce cell death through apoptosis. Judging from its characteristics, AgNP-ORPE has a good level of stability as an anti-cancer agent. This is also seen from its so potential to inhibit the growth of colon cancer cells (*in vitro*) at a fairly high percentage. However, further studies still need to be carried out to provide a stronger basis regarding the use of Okra extract in inhibiting the growth of colon cancer cells.

Acknowledgements

The author would like to thank the Rajawali Health Institute, Airlangga University, Indonesia and the Education Fund Management Institute of the Ministry of Finance of the Republic of Indonesia for facilitating and funding this research.

References

[1] I Mármol, C Sánchez-de-Diego, AP Dieste, E Cerrada and MJR Yoldi. Colorectal carcinoma: A general overview and future perspectives in colorectal cancer. *Int. J. Mol. Sci.* 2017; **18**, 197.

[2] MS Padang and L Rotty. Adenokarsinoma kolon: Laporan kasus. *E CliniC* 2020; **8**, 229-36.

[3] American Cancer Society. *Colorectal cancer facts & figures 2020-2022*. American Cancer Society, Georgia, 2022.

[4] F Bray, J Ferlay, I Soerjomataram, RL Siegel, LA Torre and A Jemal. Global cancer statistics 2018: GLOBOCAN estimates of incidence and mortality worldwide for 36 cancers in 185 countries. *CA Canc. J. Clinicians* 2018; **68**, 394-424.

[5] RM McQuade, V Stojanovska, JC Bornstein and K Nurgali. Colorectal cancer chemotherapy: The evolution of treatment and new approaches. *Curr. Med. Chem.* 2017; **24**, 1537-57.

[6] JW Kim, SW Han, JY Cho, IJ Chung, JG Kim, KH Lee, KU Park, SK Baek, SC Oh, MA Lee, D Oh, B Shim, JB Ahn, D Shin, JW Lee and YH Kim. Korean red ginseng for cancer-related fatigue in colorectal cancer patients with chemotherapy: A randomised phase III trial. *Eur. J. Canc.* 2020; **130**, 51-62.

[7] M Patwekar, N Sehar, F Patwekar, A Medikeri, S Ali, RM Aldossri and MU Rehman. Novel immune checkpoint targets: A promising therapy for cancer treatments. *Int. Immunopharm.* 2024; **126**, 111186.

[8] Y Zhang, A Rajput, N Jin and J Wang. Mechanisms of immunosuppression in colorectal cancer. *Cancers* 2020; **12**, 3850.

[9] T Hillman. Bacteriobot drug-liposome carriers: An optimization of cancer-drug delivery to the colon by manipulating the gut microbiome. *Nanoparticle* 2019; **1**, 1.

[10] MA Octavia. 2021, Aktivitas Fraksi Etanol Biji Melinjo (Gnetum gnemon L.) Terhadap Sel Kanker Kolon (WiDr) Sebagai Agen Ko-Kemoterapi. Master Thesis. Universitas Muhammadiyah, Yogyakarta, Indonesia.

[11] HA Lakshita. 2020, Aktivitas Fraksi N-Heksan Daun Binahong (Anredera Cordifolia (Tenore) Steenis) Terhadap Sel Kanker Kolon (WIDR) sebagai Agen Ko-Kemoterapi. Master Thesis. Universitas Muhammadiyah, Yogyakarta, Indonesia.

[12] YH To, K Degeling, S Kosmider, R Wong, M Lee, C Dunn, G Gard, A Jalali, V Wong, M IJzerman, P Gibbs and J Tie. Circulating tumour DNA as a potential cost-effective biomarker to reduce adjuvant chemotherapy overtreatment in stage II colorectal cancer. *Pharmacoeconomics* 2021; **39**, 953-64.

[13] RFCPA Helderman, DR Löke, J Verhoeff, HM Rodermond, GGWV Bochove, M Boon, SV Kesteren, JJG Vallejo, HP Kok, PJ Tanis, NAP Franken, J Crezee and AL Oei. The temperature-dependent effectiveness of platinum-based drugs mitomycin-C and 5-FU during hyperthermic intraperitoneal chemotherapy (HIPEC) in colorectal cancer cell lines. *Cells* 2020; **9**, 1775.

[14] KCY Huang, SF Chiang, WTL Chen, TW Chen, CH Hu, PC Yang, TW Ke and KSC Chao. Decitabine augments chemotherapy-induced PD-L1 upregulation for PD-L1 blockade in colorectal cancer. *Cancers* 2020; **12**, 462.

[15] S Hayaza, SPA Wahyuningsih, RJK Susilo, AA Permanasari, SA Husen, D Winarni, H Punnapayak and W Darmanto. Anticancer activity of okra raw polysaccharides extracts against human liver cancer cells. *Trop. J. Pharmaceut. Res.* 2019; **18**, 1667-72.

[16] MA AbuDalo, IR Al-Mheidat, AW Al-Shurafat, C Grinham and V Oyanedel-Craver. Synthesis of silver nanoparticles using a modified Tollens' method in conjunction with phytochemicals and assessment of their antimicrobial activity. *PeerJ* 2019; **7**, e6413.

[17] C Yao, L Zhang, J Wang, Y He, J Xin, S Wang, H Xu and Z Zhang. Gold nanoparticle mediated phototherapy for cancer. *J. Nanomaterials* 2016; **2016**, 5497136.

[18] S Hayaza, SPA Wahyuningsih, RJK Susilo, SA Husen, D Winarni, RA Doong and W Darmanto. Dual role of immunomodulation by crude polysaccharide from okra against carcinogenic liver injury in mice. *Heliyon* 2021; **7**, e06183.

[19] A Demange and S Fleutot. Synthesis and characterization of a silver nanoparticle- based material. *Nanoparticle* 2020; **2**, 05.

[20] H Ma, W Jiang, J Ding, M Li, Y Cheng, S Sun, C Fu and Y Liu. Polymer nanoparticle-based chemotherapy for spinal malignancies. *J. Nanomaterials* 2016; **2016,** 4754190.

[21] K Mavani and M Shah. Synthesis of silver nanoparticles by using sodium borohydride as a reducing agent. *Int. J. Eng. Res. Tech.* 2014; **2**, 1-5.

[22] S Ghazal, N Khandannasab, Hasan Ali Hosseini, Z Sabouri, A Rangrazi and M Darroudi. Green synthesis of copper-doped nickel oxide nanoparticles using okra plant extract for the evaluation of their cytotoxicity and photocatalytic properties. *Ceram. Int.* 2021; **47**, 27165-76.

[23] IMD Rosa, JM Kenny, D Puglia, C Santulli and F Sarasini. Morphological, thermal and mechanical characterization of okra (Abelmoschus esculentus) fibres as potential reinforcement in polymer composites. *Compos. Sci. Tech.* 2010; **70**, 116-22.

[24] M Hafeez, SM Hassan, SS Mughal, M Munir and MK Khan. Antioxidant, antimicrobial and cytotoxic potential of *Abelmoschus esculentus*. *Chem. Biomol. Eng.* 2020; **5**, 69.

[25] C He, L Bai, D Liu and B Liu. Interaction mechanism of okra (*Abelmoschus esculentus* L.) seed protein and flavonoids: Fluorescent and 3D-QSAR studies. *Food Chem. X* 2023; **20**, 101023.

[26] DS Kumar, DE Tony, AP Kumar, KA Kumar, DBS Rao and R Nadendla. A review on: *Abelmoschus esculentus* (OKRA). *Int. Res. J. Pharmaceut. Appl. Sci.* 2013; **3**, 129-32.

[27] Y Cui, J Wu, Y Chen, F Ji, X Li, J Yang, SB Hong, Z Zhu and Y Zang. Optimization of near-infrared reflectance models in determining flavonoid composition of okra (*Abelmoschus esculentus* L.) pods. *Food Chem.* 2023; **418**, 135953.

[28] SPA Wahyuningsih, M Pramudya, IP Putri, D Winarni, NII Savira and W Darmanto. Crude polysaccharides from okra pods (*Abelmoschus esculentus*) grown in Indonesia enhance the immune response due to bacterial infection. *Adv. Pharmacol. Sci.* 2018; **2018**, 8505383.

[29] NMA Sufyani, NA Hussien and YM Hawsawi. Characterization and anticancer potential of silver nanoparticles biosynthesized from *Olea chrysophylla* and *lavandula dentata* leaf extracts on HCT116 colon cancer cells. *J. Nanomaterials* 2019; **2019**, 7361695.

[30] J Yang, X Chen, S Rao, Y Li, Y Zang and B Zhu. Identification and quantification of flavonoids in Okra (*Abelmoschus esculentus* L. Moench) and antiproliferative activity *in vitro* of four main components identified. *Metabolites* 2022; **12**, 483.

[31] A Michalcová, L Machado, I Marek, M Martinec, M Sluková and D Vojtěch. Properties of Ag nanoparticles prepared by modified Tollens' process with the use of different saccharide types. *J. Phys. Chem. Solid.* 2018; **113**, 125-33.

[32] ST Galatage, AS Hebalkar, SV Dhobale, OR Mali, PS Kumbhar, SV Nikade and SG Killedar. Silver nanoparticles: Properties, synthesis, characterization, applications and future trends. *In*: S Kumar, P Kumar and CS Pathak (Eds.). Silver micro-nanoparticles - properties, synthesis, characterization, and applications. IntechOpen, London, 2021.

[33] SA Musthafa, K Muthu, S Vijayakumar, SJ George, S Murali, J Govindaraj and G Munuswamy-Ramanujam. Lectin isolated from Abelmoschus esculentus induces caspase mediated apoptosis in human U87 glioblastoma cell lines and modulates the expression of circadian clock genes. *Toxicon* 2021; **202**, 98-109.

[34] HT Phan and AJ Haes. What does nanoparticle stability mean? *J. Phys. Chem. C.* 2019; **123**, 16495-507.

[35] Mikhailova EO. Silver Nanoparticles: Mechanism of Action and Probable Bio-Application. *J. Funct. Biomater.* 2020; **11**, 20794983.

[36] YG Yuan, S Zhang, JY Hwang and IK Kong. Silver nanoparticles potentiates cytotoxicity and apoptotic potential of camptothecin in human cervical cancer cells. *Oxidative Med. Cell. Longevity* 2018; **2018**, 6121328.

[37] JRD Carvalho, JW Setubal, RLD Sousa, MPR D'Almeida, TN Alves, VBD Silva, IDSMD Souza and HJCD Assis. Cultivares de quiabeiro sob diferentes polinizações e seus efeitos na qualidade física e

fisiológica das sementes/ Okra cultivars under different pollinations and their effects on the physical and physiological quality of seeds. *Braz. J. Dev.* 2020; **6**, 94728-38.

[38] H Liu, Q Yao, X Wang, H Xie, C Yang, H Gao and C Xie. The research progress of crosstalk mechanism of autophagy and apoptosis in diabetic vascular endothelial injury. *Biomed. Pharmacother.* 2024; **170**, 116072.

[39] L Brice, T Girardet and S Fleutot. Nanoparticles toxicity and biocompatibility tests. *Nanoparticle* 2020; **2**, 06.